Liquid Crystals
Publication details, including instructions for authors and subscription information:
http://www.informaworld.com/smpp/title~content=t713926090

Reorientation instabilities and viscoelastic measurements in a main chain thermotropic nematic polymer Optical and NMR studies

P. Esnault[a]; J. P. Casquilho[ab]; F. Volino[a]; A. F. Martins[c]; A. Blumstein[d]
[a] Centre d'Etudes Nucléaires de Grenoble, Grenoble Cedex, France [b] Faculdade de Ciĕncias e Tecnologia, Universidade Nova de Lisboa, Portugal [c] Centro de Fisica da Materia Condensada, INIC, Lisboa Cedex, Portugal [d] Polymer Science Program, Department of Chemistry, University of Lowell, Lowell, Massachusetts, U. S. A.

To cite this Article Esnault, P. , Casquilho, J. P. , Volino, F. , Martins, A. F. and Blumstein, A.(1990) 'Reorientation instabilities and viscoelastic measurements in a main chain thermotropic nematic polymer Optical and NMR studies', Liquid Crystals, 7: 5, 607 — 628
To link to this Article: DOI: 10.1080/02678299008036746
URL: http://dx.doi.org/10.1080/02678299008036746

LIQUID CRYSTALS, 1990, VOL. 7, NO. 5, 607–628

Reorientation instabilities and viscoelastic measurements in a main chain thermotropic nematic polymer

Optical and NMR studies

by P. ESNAULT, J. P. CASQUILHO† and F. VOLINO‡
Centre d'Etudes Nucléaires de Grenoble, DRF/SPh/PCM, 85X,
38041 Grenoble Cedex, France

A. F. MARTINS
Centro de Fisica da Materia Condensada, INIC, Avenida Gama Pinto-2,
1699 Lisboa Cedex, Portugal

and A. BLUMSTEIN
Polymer Science Program, Department of Chemistry University of Lowell, Lowell,
Massachusetts 01854, U.S.A.

(*Received 6 October 1989; accepted 24 November 1989*)

The reorientational behaviour of a nematic monodomain, in a static magnetic field, following the rotation of the mean director through an angle $\alpha \approx \pi/2$ to the magnetic field direction, is investigated by optical polarizing microscopy and proton NMR spectroscopy. Optical evidence supporting a reorientation process through a pure bend transient distortion of the director field is reported for poly (4,4′-dioxy-2,2′-dimethylazoxybenzene nonanediyl), a main-chain nematic thermotropic polymer. The time evolution of the distortion and flow patterns are deduced from a detailed analysis of the NMR lineshapes recorded during the reorientational process. The viscosity coefficients γ_1, α_1, α_2, η_c and the ratio K_3/K_1 of the bend to splay Frank elastic constants are determined and discussed in terms of the existing theories.

1. Introduction

The mechanical properties of liquid crystal polymers are an important aspect of their technological interest. In recent years, much work has been carried out in order to understand the specific viscoelastic behaviour of these materials, whose nature is both polymeric and liquid-crystalline. According to this dual aspect, the studies that have been performed can be classified approximately into two groups: (1) rheological studies as applied in the field of conventional flexible polymeric systems which lead, in particular, to the determination of a shear viscosity, both in the nematic and isotropic phases [1, 2, 3, 4], (ii) liquid-crystalline type approaches whose challenge is the determination of the five Leslie viscosity coefficients and of the three Frank

† On leave from Faculdade de Ciências e Tecnologia, Universidade Nova de Lisboa, Portugal.
‡ Member of CNRS.

0267–8292/90 $3.00

elastic constants [5] which are needed, in the framework of the Ericksen–Leslie–Parodi theory [6, 7, 8], to describe the hydrodynamic and viscoelastic behaviour of liquid-crystalline materials in the nematic phase. Along this second route, important work has been done, both on theoretical [9, 10, 11] and experimental aspects [12, 13], mainly for lyotropic systems. Experimental studies of the viscoelastic properties of thermotropic main-chain polymers are far more scarce [14, 15, 16]. Recently, we have proposed an NMR method to measure four of the five viscosity coefficients of a main-chain thermotropic nematic polymer [16]. This method is based on the quantitative description of the reorientation process, in a static magnetic field, of a nematic monodomain whose mean director has been removed from its equilibrium position by rotation through an angle α. The relaxation of the director field towards equilibrium has been observed to be qualitatively different for initial rotation of $\alpha < \pi/4$ and $\alpha > \pi/4$ [17, 18]. The well known homogeneous relaxation which occurs for $\alpha < \pi/4$ leads to the determination of the twist viscosity coefficient, γ_1 [19]. Previous work has used this method widely for systematic studies of this coefficient as a function of temperature and molecular mass of the polymer [15–20]. The reorientation process which takes place for $\alpha > \pi/4$ is more complex. The model which was developed in [16] describes this process for $\alpha \sim \pi/2$. In this case, it appears that the easiest path towards equilibrium involves a spatially periodic, transient distortion of the director field coupled with backflow effects. It can be derived from the Ericksen–Leslie–Parodi equations that such distortion induces a considerable lowering of the effective viscosity coefficient which drives the reorientation. It can be noted that these field-induced transient structures occuring in the bulk of the sample belong to the same class of phenomena studied theoretically [21, 22] and observed experimentally by optical techniques on comparatively thin planar samples of oriented low molecular mass liquid crystals [22, 23] and lyotropic polymeric systems [24, 25]. Recent comments have been made [26] regarding the geometry of the selected distortion which was assumed in [16]. The first aim of this paper is to report optical evidence for the geometry of the period structure for poly (4,4′-dioxy-2,2′-dimethylazoxybenzene nonanediyl), a main-chain nematic thermotropic polymer of the Me9Sn series [27] studied in this paper. Then, after a brief return to the model developed in [16], we describe extensively an improved NMR method, based on a detailed analysis of the NMR lineshapes, to refine the viscosity measurements and to evaluate more accurately the elastic contribution to the reorientation process. It will be shown, that the model proposed in [16] provides, through the simulation of the NMR spectra, a good description of the experimental data. Some additional results concerning the hydrodynamic pattern during the relaxation will be reported and finally the viscoelastic parameters will be determined and discussed in terms of existing theories.

2. Material and method

Polymers of the Me9Sn series [27] are main-chain thermotropic polyesters of general formula:

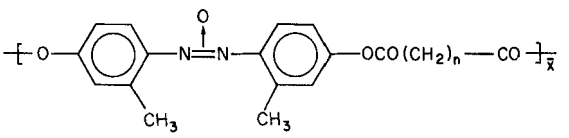

with n = 3–18 and $\bar{x}$ the average number of repeat units. They are based on a regularly alternating rigid mesogens (R) and flexible spacers (F). The polymer with

$n = 10$ has been studied previously in [16]. The polymer with $n = 7$ will be considered in this work and hereafter labelled AZA9. Two samples were used for the present study: a conventional, fully hydrogenated AZA9 polymer for the optical observation ($\bar{M}_n = 7300$, $\bar{x} \approx 18$, $T_{NI} \approx 142°C$) and a spacer deuteriated polymer AZA9d14 for the NMR study ($\bar{M}_n = 4300$, $\bar{x} \approx 10$, ($T_{NI} \approx 132°C$).

The polymer sample was first annealed in the pure isotropic phase for about 20 min, at about 15°C above T_{NI}, and then cooled rapidly at the desired temperature, in the magnetic field of the NMR spectrometer (Brüker CXP90). After enough time, an equilibrium state is reached and a nematic monodomain is obtained: the macromolecules are aligned, on average, parallel to the magnetic field. The optic axis $\mathbf{n}_0$ lies along the magnetic field. The proton NMR (PMR) spectrum of the polymer (see figure 4 (*a*) exhibits a doublet whose splitting δ_0 reflects the macroscopic alignment of the polymer, as well as its degree of order. At $t = 0$, the tube containing the sample is suddenly rotated through an angle $\alpha \approx \pi/2$ about an axis normal to the plane defined by the magnetic field **H** and the mean director $\mathbf{n}_0$ in order to achieve $\mathbf{n}_0$ perpendicular to **H**. This situation is a non-equilibrium state. So for $t > 0$, the nematic director relaxes back to equilibrium. The reorientation process is followed by recording PMR spectra as a function of time. After enough time, the initial situation $\mathbf{n}_0$ parallel to **H** is recovered.

3. Optical study

3.1. *Experimental*

This experiment was performed with an AZA9 polymer sample prepared in an NMR tube whose cross section was previously weakly ovalized ($2a \approx 6{\cdot}1$ mm, $2b \approx 3{\cdot}5$ mm (see figure 1 (*a*)). This geometry of the tube allows us to distinguish the relevant directions within the sample. At $t = 0^-$, the sample is at rest in the magnetic field **H**, so that the mean director $\mathbf{n}_0$, the magnetic field **H** and the main axis **a** of the elliptical section are colinear. At $t = 0$, just after rotation **H** lies along the small axis **b** (see figure 1 (*b*)). For $t > 0$, the relaxation process is followed in real time by observing the free induction decay curve on the oscilloscope of the spectrometer. At a given time of the reorientation, defined as the time when the corresponding NMR lineshape is observed to be the narrowest (most of the molecules within the sample make an average angle $\sim 54°$ with the magnetic field direction, see the NMR section), the sample is suddenly removed from the magnetic field and quenched into freezing water. Due to the large increase in the viscosity obtained by decreasing the temperature [15, 20], the periodic structure existing in the sample at that time is expected to be frozen in a glassy state. Then, the polymer is carefully released from the NMR tube, embedded in a rapidly setting epoxy resin and cut with a microtome under refrigerating conditions (nitrogen gas flow) along the direction defined in figure 1 (*c*). Slice (1) is a transversal section of the tube perpendicular to the axis of the tube **t**, and contains the initial direction of alignment $\mathbf{n}_0$ and the reorientating field **H**. Slice (2) is chosen perpendicular to **H**. The typical thickness of the slices is about $\sim 10\,\mu$m; they were observed under a polarizing microscope (Olympus BH2).

3.2. *Results and discussion*

Figure 2 (*a*) shows a typical photomicrograph of a slice of type (1) (magnification $\times 50$) with parallel polarizer and analyser: a well-defined structure with alternating bright and dark stripes parallel to the small axis **b** of the elliptical section of

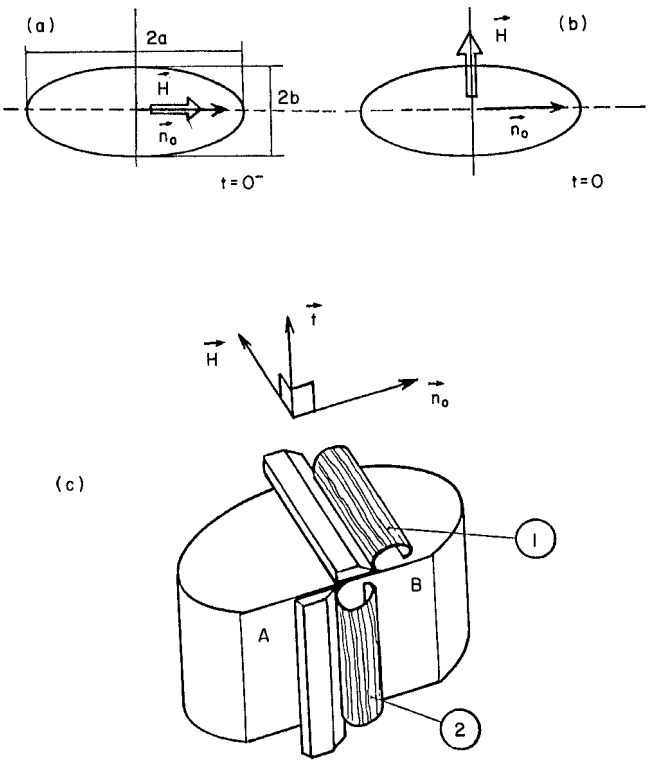

Figure 1. Sketch of the reorientation conditions used in the optical experiment. Views of the elliptical section of the NMR tube: (*a*) sample at rest in the magnetic field ($\mathbf{n}_0 \parallel \mathbf{H}$), (*b*) after rotation of the magnetic field $\mathbf{n}_0$, by an angle of $\sim \pi/2$ ($\mathbf{n}_0 \perp \mathbf{H}$), (*c*) schematic representation of the cutting directions for the quenched sample: slice (1) contains the directions $\mathbf{n}_0$ and **H**; slice (2) is perpendicular to **H**.

the sample, i.e. perpendicular to the initial direction of alignment $\mathbf{n}_0$, is observed. Such a result is obtained whatever the cutting direction with respect to $\mathbf{n}_0$. The spacing between stripes corresponds to a wavelength of 50–70 μm. This modulation of the nematic medium is slightly modified by rotation of the polarizer; however a complete exchange between dark and bright lines is not observed, probably because of the thickness of the slice. Figure 2 (*b*) shows a photomicrograph of an equivalent slice obtained for a macroscopically aligned sample whose mean director has not been perturbed by rotation in the magnetic field. In this case, no stripes are observed at the same magnification ($\times$ 50). This experiment proves that the stripe structure is not induced by the shear of the microtome blade in the surface sample. Figure 2 (*c*)

Figure 2. Typical photomicrographs viewed under a polarizing microscope (analyser and polarizer at 0°) obtained for quenched samples of the AZA9 polymer: (*a*) slice (1) during the reorientation process: alternative bright and dark stripes perpendicular to $\mathbf{n}_0$ are observed; (*b*) slice (1) at rest in the magnetic field: no stripes are observed; (*c*) slice (2) during the reorientation process: alternative dark and bright stripes perpendicular to $\mathbf{n}_0$ are observed. The segment *A*–*B* which separates the dark part (epoxy matrix) from the clear part (AZA9 polymer) of the sample defines the trace of the ($\mathbf{n}_0$, **H**) plane. In (*a*) and (*c*), the spacing between equivalent stripes is 50–80 μm.

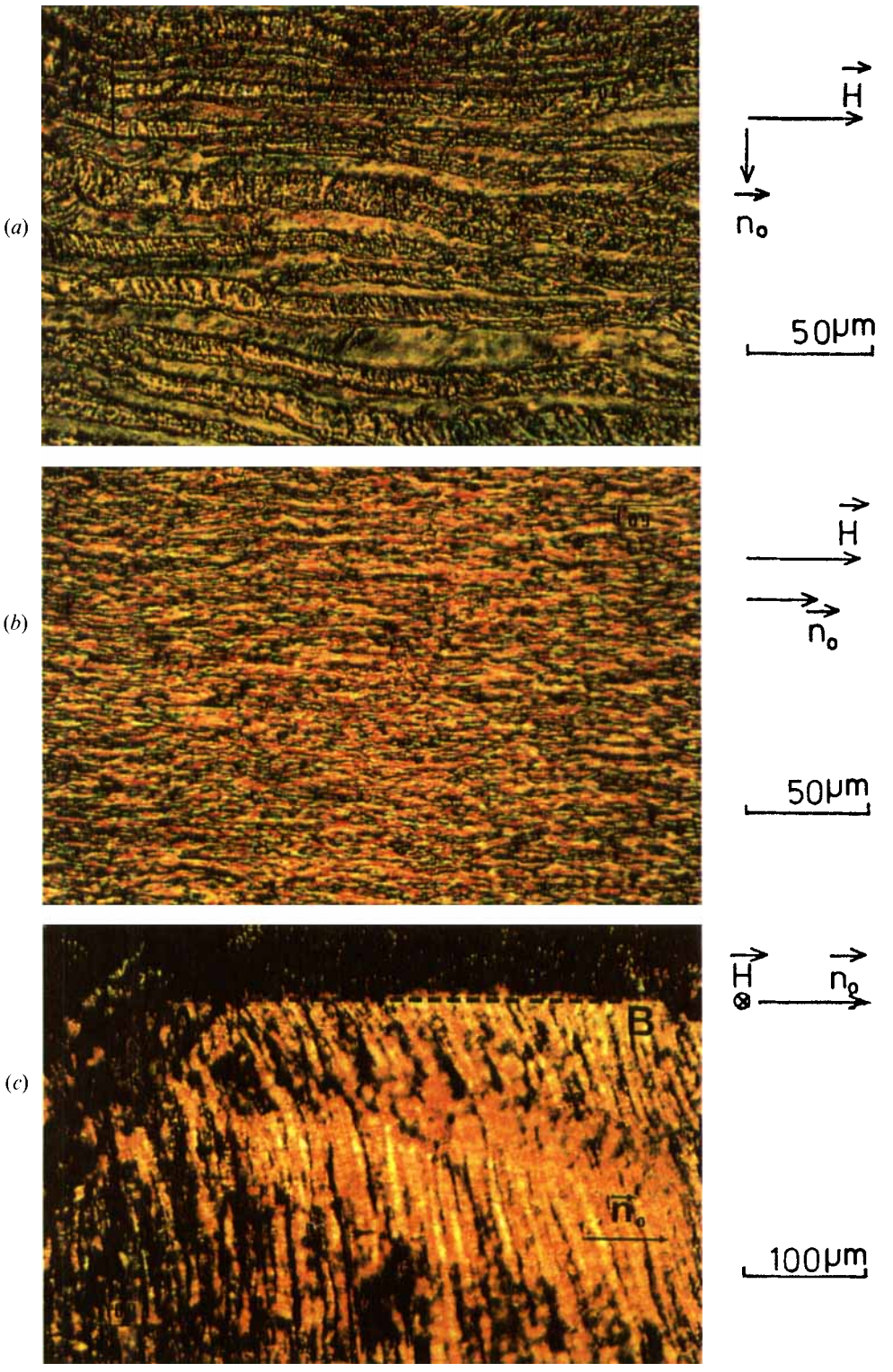

shows a typical photomicrograph of one slice of type (2) (× 20). Stripes perpendicular, on average, to the plane ($\mathbf{n}_0$, $\mathbf{H}$), that is to the plane of section (1), whose trace is represented by segment AB in figure 2 (*c*), are observed. The spacing between stripes is about the same as in slice (1).

These observations clearly indicate that the director field is homogeneous along the direction of the magnetic field. This definitely excludes the hypothesis of a splay-bend transient reorientation instability. Indeed, in this case, an oblique set of stripes characterized by two wavevector components, parallel and perpendicular to the initial direction of alignment $\mathbf{n}_0$, would have been observed in slice (1) [25]. Secondly, homogeneity of the director field along the main axis of the tube is also observed, suggesting that the twist component of the wavevector of the distortion along this axis can be neglected (oblique stripes would have been observed in slice (2) if any [26]). It can be concluded from these results that, in this 5 mm diameter NMR tube, the reorientation of the mean director subsequent to rotation of the magnetic field through $\alpha = \pi/2$ occurs via a periodic transient instability of the director field whose wavevector lies along the initial direction of alignment $\mathbf{n}_0$: this defines a *pure bend* distortion [19].

Of course, it would have been very instructive to follow directly the full evolution of the instability, and in particular the conditions of its nucleation. This is, unfortunately, not possible with this sample due to the opacity of the material. However, comparison with similar experiments is instructive. We have observed in identical NMR tubes, magnetic reorientation stripes in samples of nematic solutions of polybenzyl-l-glutamate originating from the bottom of the tube, with a wavelength much smaller than the tube diameter. In nematic solutions of tobacco mosaic virus, both the nucleation by the boundaries and by thermal fluctuations far from the boundaries have been observed, the former ones developing at a faster rate than the latter [25]. This suggests strongly that in our polymer, the stripe development mechanism is based on boundary effects.

The description via a unique formalism of the nucleation process and growth of the instability is a very complicated problem that has not yet received a complete solution, even in the simplest case of the twist geometry. The nucleation problem in this geometry has been treated only very recently by Srajer *et al.* [48] and that of the evolution by Rey and Denn [49]. In [16] a model was developed to describe the evolution in the geometry of our experiment, assuming that the initial state is a pure bend distortion of very small, but finite, amplitude and that the fundamental wavelength of this distortion does not change with time. The former assumption is well supported by the optical observations. The latter assumption may be more questionable because the results of [48] show an increase of the wavelength. This increase is, however, not large (about 30 per cent) and the assumption of a constant wavelength (which constitutes a limitation of the model) is sufficient for our purpose (see section 5.3).

In the next section, we present briefly the main results of this model (developed in [16]) which will be used in this paper to examine the influence of this distortion on the NMR lineshapes.

4. Theoretical background

The initial rotation α of the NMR sample is performed counterclockwise around the axis $\mathbf{t}$ of the (cylindrical) NMR tube defined as the y axis of a laboratory frame. The z axis is taken as the initial direction of the mean direction $\mathbf{n}_0$. Thus, after

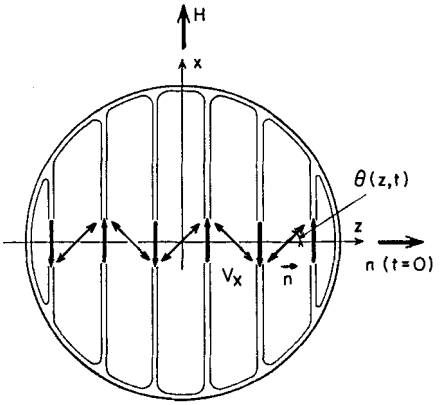

Figure 3. Schematic representation of the NMR tube section. The initial alignment direction $\mathbf{n}_0$ defines the z axis. For $t > 0$, a periodic pure bend transient distortion develops with adjacent domains rotating in opposite directions and backflow induced along the magnetic field direction. The local directors within the sample make an angle $\theta(z, t)$ with the z axis.

rotation, at $t = 0$, the magnetic field **H** lies along the x axis (see figure 3): we have $\mathbf{H} \equiv (H, 0, 0)$ and $\mathbf{n}_0 \equiv (0, 0, 1)$. For $t > 0$, according to the observations reported here, a pure bend structure of wavenumber q develops along the z-axis producing opposite rotations of the directors separated by a distance π/q, whereas backflow is induced parallel to the x axis: $v_x(t > 0) \neq 0$ (see figure 3). Neglecting the y dependence of the director and velocity fields $\mathbf{n}(\mathbf{r})$ and $\mathbf{v}(\mathbf{r})$ (no twist), as well as the surface effects (infinite boundary conditions), the Eriksen–Leslie–Parodi equations can be solved. This leads to a set of coupled equations for the director and velocity fields. Assuming that the inertial terms can be neglected with respect to the viscous ones, which is equivalent to saying that the short initial acceleration time τ_{acc} is over when the process which is described here starts [28, 29], (a well justified assumption for our system: see the discussion) and taking into account the periodicity of the velocity and director fields along the z axis, the equations

$$\left(\gamma_1 - \frac{j^2(\theta)}{g(\theta)}\right)\frac{\partial\theta}{\partial t} - \tfrac{1}{2}\chi_a B^2 \sin 2\theta - K(\theta) = 0 \tag{1}$$

$$\frac{\partial v_x}{\partial z} = -\frac{j(\theta)}{g(\theta)}\frac{\partial\theta}{\partial t} \tag{2}$$

are obtained [16] where $\theta = \theta(\mathbf{r}, t)$ is the angle between the director at point **r** and time t and the z axis of the reference frame (see figure 3) χ_a is the anisotropy of the magnetic susceptibility per unit volume, **B** is the magnetic flux density and

$$K(\theta) = f(\theta)\frac{\partial^2\theta}{\partial z^2} + \frac{1}{2}\left(\frac{\partial f(\theta)}{\partial\theta}\right)\left(\frac{\partial\theta}{\partial z}\right)^2, \tag{3}$$

$$f(\theta) = K_1 - (K_1 - K_3)\cos^2\theta, \tag{4}$$

$$j(\theta) = \alpha_2 - \gamma_2 \sin^2\theta, \tag{5}$$

$$g(\theta) = (\alpha_1 \cos^2\theta + \gamma_2)\sin^2\theta + \eta_c, \tag{6}$$

where α_1, α_2, $\gamma_2 = \gamma_1 + 2\alpha_2$, and η_c are the usual nematic viscosities; the convention of [19] is adopted.

The differential equation (1), which is strongly non-linear, is quite similar to that derived for the homogeneous relaxation process [19] except that the twist viscosity coefficient $\eta_{\text{twist}} = \gamma_1$ needed in the latter is now replaced by an effective viscosity coefficient

$$\gamma_{\text{eff}} = \gamma_1 - j^2(\theta)/g(\theta).$$

In addition, an elastic contribution $K(\theta)$ is needed due to the distortion of the director field. Equation (1) may be simplified by taking the harmonic approximation to the z dependence of the function $\theta(z, t)$

$$\theta(z, t) = \theta_0(t) \sin qz; \tag{7}$$

Then

$$\frac{\partial^2 \theta}{\partial z^2} = -q^2\theta \quad \text{and} \quad \left(\frac{\partial \theta}{\partial z}\right)^2 = q^2(\theta_0^2 - \theta^2). \tag{8}$$

Solving equation (1), taking into account equations (7) and (8) in the limit $\theta \to 0$, allows us to derive the initial characteristic time of the process τ_i in the harmonic approximation

$$\tau_i = \eta_{\text{bend}}/(\chi_a B^2 - K_3 q^2), \tag{9}$$

where $\eta_{\text{bend}} = \gamma_1 - \alpha_2^2/\eta_c$ is the viscosity coefficient associated with the pure bend elastic modes [30]. For comparison, the characteristic time derived for an homogeneous reorientation process is given by [19]

$$\tau_0 = \eta_{\text{twist}}/\chi_a B^2. \tag{10}$$

Now, in order to deduce the viscosity and elastic parameters involved in equation (1), we have to detail how the information $\theta(z, t)$ can be extracted from the NMR lineshapes and compared to equation (1).

5. NMR results

The AZA9d14 polymer with a deuteriated spacer has been used in the NMR experiments. Indeed, due to the deuteriation of the spacer, the PMR spectrum of this polymer is more structured and thus more suitable for lineshape analysis than that of the fully protonated polymer. A deep understanding of the equilibrium NMR lineshapes is indeed required to achieve the relevant simulations. A detailed study of the equilibrium lineshape has been performed, for this polymer, in a previous paper [31]. The upper spectrum in figure 4 is a typical PMR spectrum of the AZA9d14 polymer macroscopically aligned in the magnetic field (120°C). The other spectra in figure 4 are those obtained as a function of time, during the reorientation process following a rotation through $\alpha = \pi/2$ (the typical acquisition time for one spectrum is a few seconds). It can be noted that the reorientation strongly affects the shape of the spectra. The reorientation being slow (minutes typically), the distortion of the nematic medium can be considered as a static deformation during the acquisition time. Consequently, the NMR lines reflect the local director desorientations with respect to the magnetic field direction and therefore the distortion shape. Let us discuss this point in more quantitative manner.

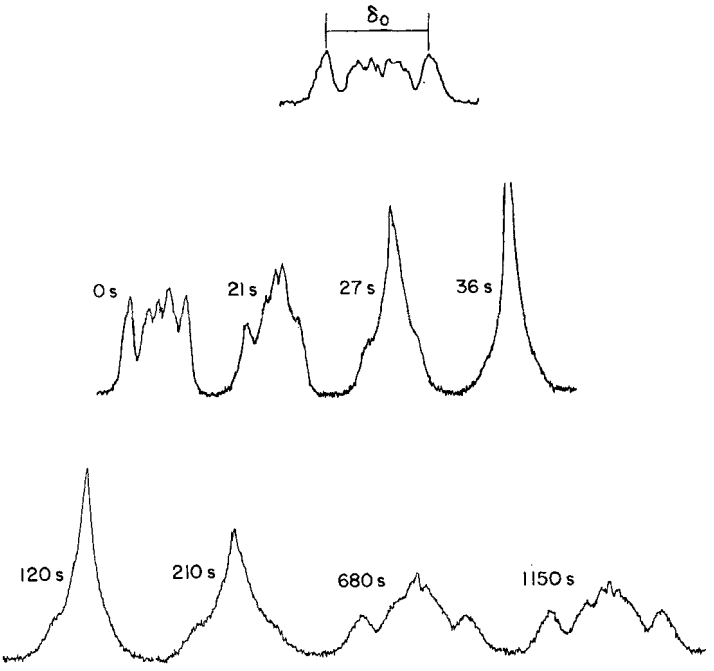

Figure 4. Set of typical PMR spectra of the AZA9d14 polymer recorded as a function of time during the reorientation process following a rotation of the sample ($\alpha = \pi/2$. $T = 120°C$). Note the very drastic change in lineshape. The upper spectrum is the equilibrium spectrum before rotation. The splitting δ_0 is related to the nematic order parameter S by equation (16).

5.1. *NMR lineshapes and distortion of the director field*

Let $f_0(\nu)$ be the NMR spectrum of the polymer, macroscopically aligned in the magnetic field (see figure 4(*a*)). Immediately after the rotation of **H** through some angle α, the director field $n(\mathbf{r})$ remains homogeneous in space ($\theta(z, 0) = 0$). This can be checked easily by recording a new spectrum after a subsequent rotation of $-\alpha$: this spectrum is found to be identical to the initial one. So, only the angle between $\mathbf{n}_0$ and **H** changes when going from zero to α. Thus, the NMR spectrum $f_\alpha(\nu, t = 0) = f_\alpha(\nu, 0)$ recorded immediately after rotation is, *a priori*, expected to have exactly the same shape as before, except for a scaling factor

$$f_\alpha(\nu, 0) = \frac{1}{P_2(\cos\alpha)} f_0\left(\frac{\nu}{P_2(\cos\alpha)}\right), \tag{11}$$

where $P_2(\cos\alpha)$ is the second Legendre polynomial. In fact, the spectrum recorded under these conditions is significantly different from that expected from relation (11). It was argued in [31] that this difference originates from the contribution of the thermally excited orientation fluctuations of the director field which are not averaged on the NMR time scale [31, 32], mainly due to the high viscosity of the polymeric compounds. It has been shown, through simulation of the lineshapes for several angles α, that $f_\alpha(\nu, 0)$ is given by

$$f_\alpha(\nu, 0) = \int \frac{1}{P_2(\cos\lambda)} f_0\left(\frac{\nu}{P_2(\cos\lambda)}\right) F_s(\Omega) d\Omega, \tag{12}$$

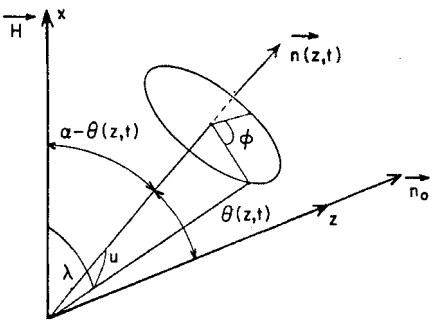

Figure 5. Definition of the various angles used in equations (12) and (14). α is the angle between the initial direction of alignment $\mathbf{n}_0 = z$ and the reorienting magnetic field $\mathbf{H} = x$. The polar and azimuthal angles u and φ, describe the static disorientation around the local director $\mathbf{n}(z, t)$. $\theta(z, t)$ is the angle between the director $\mathbf{n}$ at point r, and the z axis, at time t of the reorientation process.

where Ω denotes the orientation of the local static director about the mean director (polar angle u, azimuthal angle φ), and λ is the angle between the field and local director given by

$$\cos\lambda = \sin u \sin\alpha \cos\varphi + \cos u \cos\alpha.$$

The angles λ, u, φ, α are sketched in figure 5. $F_s(\Omega)$ follows the simple functional form, with cylindrical symmetry [31]

$$F_s(\Omega) = Z^{-1} \exp(A \cos^2 u), \tag{13}$$

where Z is a normalisation constant and A an adjustable parameter. The constant A or equivalently, the static order parameter S_{stat} defined by

$$S_{stat} = \int P_2(\cos u) f_s(\Omega) d\Omega,$$

quantifies the static (on the NMR time scale) disorder of the local directors around the mean director $\mathbf{n}_0$. At $T = 120°C$, the best value of A obtained [31] for the AZA9d14 polymer is 40, corresponding to $S_{stat} = 0{\cdot}962$.

When a macroscopic distortion of the nematic medium develops, the angle between the directors at the various points of the sample and the magnetic field is no longer constant (see figure 3) and is equal, at point $\mathbf{r}$, and for a pure bend distortion, to $\alpha - \theta(z, t)$. So, the lineshape $f_\alpha(\nu, t)$ which is observed at a given time, results from the superposition of elementary spectra $f_{\alpha-\theta}(\nu)$ (see equation (12)) characteristic of the local orientation of the nematic director $\mathbf{n}(\mathbf{r}, t)$, at point $\mathbf{r}$, with respect to the magnetic field. With $\mathbf{n}(\mathbf{r}, t)$ periodic and depending only on z, we have

$$f_\alpha(\nu, t) = \frac{1}{Z} \int_0^\pi \frac{d(qz)}{\pi} \int_0^{2\pi} d\varphi \int_0^\pi du \, \frac{1}{P_2(\cos\lambda)} f_0\left(\frac{\nu}{P_2(\cos\lambda)}\right) e^{(A\cos^2 u)} \sin u, \tag{14}$$

with

$$\cos\lambda = \sin u \sin[\alpha - \theta(z, t)] \cos\varphi + \cos u \cos(\alpha - \theta(z, t)).$$

As an illustration of the effects on the NMR lineshape of the different contributions, namely distortion of the director field and static distribution $F_s(\Omega)$, figure 6 shows simulated spectra of AZA9d14 at 120°C which would be observed if

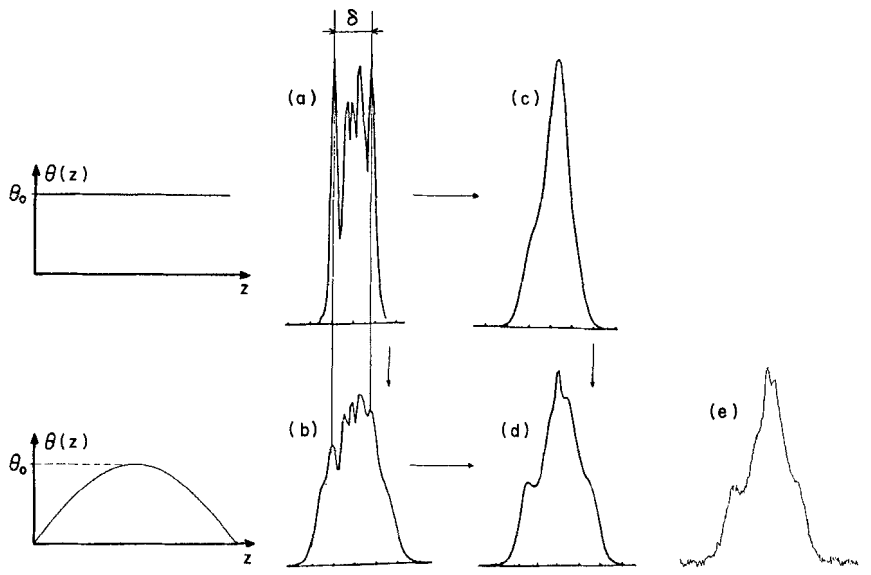

Figure 6. P.M.R. spectra of the AZA9d14 polymer simulated from equation (14) ($\alpha = \pi/2$): (*a*) $\theta(z) = 24°$, $A = \infty$; (*b*) $\theta(z) = \theta_0 \sin qz$, $\theta_0 = 24°$, $A = \infty$; (*c*) $\theta(z) = 24°$, $A = 40$; (*d*) $\theta(z) = \theta_0 \sin qz$, $\theta_0 = 24°$, $A = 40$; (*e*) experimental spectrum obtained at $t = 24$ s following the $\pi/2$-rotation. Comparison between (*d*) and (*e*) allows us to conclude that both distortion and static director distribution are needed to achieve correct simulations.

the following conditions were fulfilled:

(*a*) $\theta(z) = \theta_0 = 24°$ independent of z (no distortion, i.e. homogeneous relaxation) and $S_{stat} = 1$ (no broadening due to the static director distribution). The scaling factor in equation (11) is observed in the simulated lineshape, the main splitting δ is proportional to $P_2(\cos(\alpha - \theta))$ with $\alpha = \pi/2$, that is $\delta = \delta_0 P_2(\cos(\pi/2 - \theta))$. Therefore, in this idealized case, homogeneous relaxation reorientation process could simply be followed through the evolution of δ, which reflects directly the evolution of θ with time [15].

(*b*) $\theta(z) = \theta_0 \sin qz$ with $\theta_0 = 24°$ and $S_{stat} = 1$ (distortion but no static director distribution). In this case, a continuum of splittings δ should be observed according to the relation $\delta = \delta_0 P_2(\cos(\alpha - \theta(z))$. In fact, the $|P_2|$ function varies slowly around $\pi/2$ and remains practically equal to 1/2 for $\pi/2 \pm 10°$. So, the domains whose local directors are still close to the initial direction of alignment will contribute to the outer shoulders that are observed, whose splitting is $\sim \delta_0/2$. On the other hand, the domains whose local directors are close to θ_0 will contribute to the inner doublet whose splitting is $\sim \delta_0 P_2[\cos(\pi/2 - \theta_0)]$.

(*c*) $\theta(z) = \theta_0 = 24°$ and $S_{stat} = 0{\cdot}962$ (no distortion, but static director distribution). The spectrum is significantly different from the spectra calculated in (*a*), due to the strong variation of the $|P_2|$ factor around $\pi/2 - 24° = 66°$. Thus, a large broadening is observed which blurs the characteristic structure of the reference spectrum. The shoulders are reminiscent of the main splitting δ observed in (*a*).

(*d*) $\theta(z) = \theta_0 \sin qz$ with $\theta_0 = 24°$ and $S_{stat} = 0{\cdot}962$ (both distortion and static director distribution). The spectrum is now significantly affected. It is very different from the spectra which would be obtained for a homogeneous reorientation process ((*a*) and (*c*)). Figure 6(*e*) illustrates an experimental spectrum of AZA9d14 recorded at $t = 24$ s from the beginning of the relaxation ($\alpha = \pi/2$). The similarity with the simulated spectrum in figure 6(*d*) is striking. It can be concluded that both distortion and static director distribution are required in order to achieve correct simulations of the experimental lineshapes. Conversely, provided that S_{stat} has been measured in a previous experiment [31], the experimental distortion (shape and amplitude θ_0) can be extracted at every time of the relaxation, from simulation of the PMR lineshapes using equation (14), and by comparison with the experimental spectra.

This analysis has been extended to an empirical distortion of the form $\theta(z, t) = \theta_0(t)(\sin qz)^\beta$, with the exponent β ranging between 1 and 0, to describe a possible change in the distortion shape from sinusoidal to a square wave during the relaxation. Detailed studies have been performed to visualize the modification of the NMR lineshapes as a function of the shape (through the parameter β) and the amplitude (through θ_0) of the distortion [33], for all times during the $\alpha = \pi/2$ relaxation. The best simulations obtained by using this procedure are presented in figure 7. ($T = 120°C$, $S_{stat} = 0{\cdot}962$). From these results, values of θ_0 and β are deduced as a function of time. The experimental β is found to decrease from 1 down to 0·3 between 0 to about 1200 s. This behaviour indicates that the distortion shape is not constant but evolves roughly from an harmonic towards a square shape. So, as the reorientation proceeds, the elastic energy associated with the distortion of the director field becomes more confined in walls located close to the nodes of the distortion. The values of $\theta_0(t)$ obtained by this procedure are plotted in figure 8. As previously reported [16], a fast reorientation regime is observed at short times.

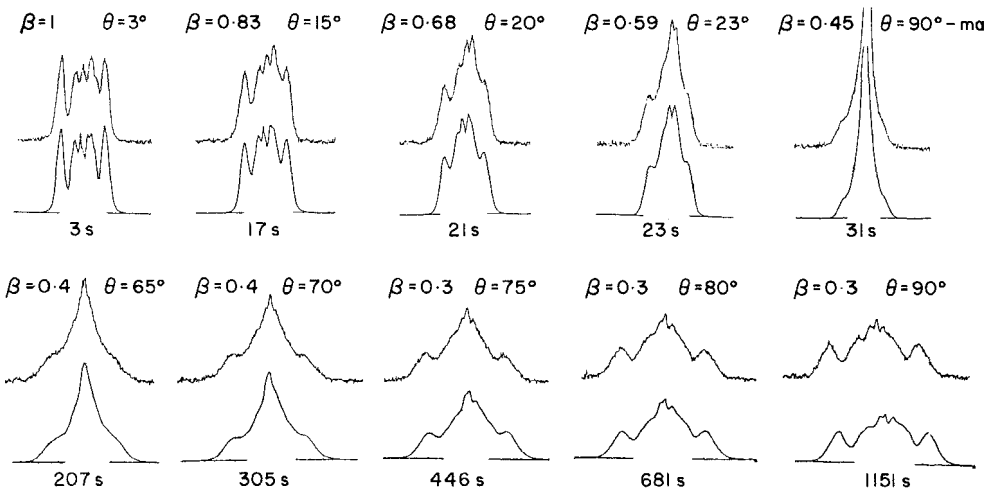

Figure 7. Experimental PMR spectra of AZA9d14 (upper) and the best simulated spectra using an empirical distortion shape of the general form: $\theta(z, t) = \theta_0(t)(\sin qz)^\beta$. Values for β and θ_0 deduced from this analysis are given for every spectrum.

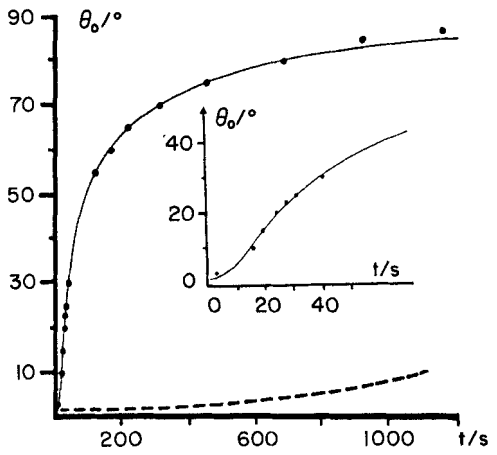

Figure 8. Amplitude θ_0 of the director distortion as a function of time deduced from the lineshape analysis shown in figure 7. The inset details the results for short times. The solid line is a typical fit of equation (1) within the harmonic approximation, with the parameters: $\alpha_1 = -14{\cdot}5\,\text{kP}$, $\alpha_2 = -16{\cdot}26\,\text{kP}$, $\eta_c = 17{\cdot}03\,\text{kP}$, $\gamma_1 = 15{\cdot}7\,\text{kP}$, $K_3/K_1 = 0{\cdot}3$, $K_1q^2 = 1\,\text{erg/cm}^3$ ($T = 120°\text{C}$). The dashed line shows the expected behaviour of $\theta_0(t)$ for the hypothesis of a homogeneous reorientation process governed by $\gamma_1 = 15{\cdot}7\,\text{kP}$.

5.2. *Fitting procedure*

This analysis shows that, by using relation (14), the experimental lineshapes can be reproduced at every time of the reorientation, at least with an empirical distortion shape. However, this shape is not related to the viscoelastic parameters of the material. Determination of these parameters requires the simulation of the time dependent NMR spectra using the distortion shape *calculated from equation (1)*. A rigorous analysis would require adjustment of the six parameters of the problem, namely γ_1, α_1, η_c, α_2, K_1q^2, K_3/K_1, by comparison of the experimental lineshapes at every time with the calculated lineshapes. These spectra would be calculated at the corresponding time by using the distortion $\theta(z, t)$ calculated through equation (1) by amplification of an initial orientational fluctuation. In fact, such a procedure, as applied on a computational level, is prohibitively time consuming and so the following three step procedure has been adopted.

(1) In order to reduce the number of parameters, the twist viscosity coefficient γ_1 is measured in a prior experiment with $\alpha < \pi/4$, through the determination of τ_0 (see equation (10)).

(2) A numerical fit of the determined values of $\theta_0(t)$ (see figure 8) is then achieved by using equation (1) within the harmonic approximation (the elastic contribution is calculated according to equation (7)) and by keeping constant the value of γ_1. The results previously published in [16] originate from this procedure. This approximation is sufficient to estimate three viscosity coefficients, namely α_1, α_2, η_c, to a good accuracy, especially α_2 and η_c. Indeed, at the beginning of the relaxation, the elastic torque $K(\theta)$ is small compared to the magnetic torque

$$H(\theta) = \tfrac{1}{2}\chi_a B^2 \sin 2\theta.$$

At the maximum of the distortion where $\theta(z, t) = \theta_0(t)$ we have, at short time,

$$K(\theta_0)/H(\theta_0) \sim K_3q^2/\chi_a B^2 \leqslant 5\text{–}10 \text{ per cent}$$

(see later). Therefore, the fit is weakly sensitive to the actual value of K_3 and consequently to the ratio K_3/K_1 (as previously reported in [16]). Thus, the evolution of $\theta_0(t)$ with time, at short times, results essentially from the competition between the magnetic and the viscous torques. This is no longer the case at the end of the relaxation where the elastic and magnetic torques become of comparable magnitude, so that the fit is expected to be sensitive to the actual value of $K_1 q^2$. Thus, the procedure used here, leads obviously to a poor evaluation of this elastic parameter, because the assumption that the distortion shape is sinusoidal during the whole process is not correct (see figure 7). An approximate estimate of the error can be made by taking into account the difference between the imposed distortion $\theta_0 \sin qz$ and the empirically evaluated distortion $\theta_0(\sin qz)^\beta$ with β ranging between 0 and 1. It can be easily shown, by considering equations (3) and (4) that the elastic energy $K_1 q^2$ deduced from the fit is underestimated by a factor $1/\beta$, that is at least a factor 3 ($\beta = 0{\cdot}3$) at the end of the relaxation, where $\theta_0 \sim \pi/2$. The fit of $\theta_0(t)$ shown in figure 8 corresponding to this second step is performed by solving equation (1) numerically by a fourth order Runge–Kutta method. The best fit was approached by an error minimization method based on a logical combination of simplex and gradient methods. The amplitude of the initial sinusoidal fluctuation $\theta_0(0)$ was chosen to be equal to 1°.

(3) The last step involves the calculation of an initial, assumed harmonic, orientation director fluctuation (amplitude $\theta_0(0) = 1°$) using equation (1) with the set of viscosity parameters so determined, but without the harmonic approximation. The elastic contribution is now computed through equation (3) taking into account the actual evolution of the shape of the distortion. The NMR lineshapes are simulated as a function of time from the calculated distortions $\theta(z, t)$ and compared to the corresponding experimental spectra. The NMR lineshapes, for a constant value of θ_0, are affected by the change in the distortion shape resulting from the variation of the elastic parameters $K_1 q^2$ and K_3/K_1 (see later). So, this last step allows us to refine the viscosity parameters determined previously and to evaluate more accurately the elastic contribution. The fitting procedure is satisfied as soon as a set of parameters allows us to reproduce the whole set of experimental spectra as a function of time.

5.3. *Results*

The results for the AZA9d14 polymer at $T = 120°C$ are presented according to the three step procedure described previously.

(1) The determination of γ_1 was performed using the method developed in previous papers [15, 20]. The anisotropy of the magnetic susceptibility, χ_a, has been measured for the polymers of the ME9Sm series and analysed in detail in a previous work [34]. The relation

$$\chi_a = (1{\cdot}42 \pm 0{\cdot}02) \times 10^{-7} S(\rho/\mathrm{g\,cm^{-3}}), \tag{15}$$

will be adopted (neglecting the biaxiality of the orientational ordering) where S is the usual nematic order parameter and ρ is the density. S is deduced from the main dipolar splitting δ_0, according to previous studies [34, 36], from

$$\delta_0/\mathrm{kHz} = 22{\cdot}74\,S. \tag{16}$$

Assuming $\rho = 1\,\mathrm{g/cm^3}$, the results at 120°C are: $S = 0{\cdot}55$, $\chi_a B^2 = 35{\cdot}5\,\mathrm{erg/cm^3}$, $\tau_0 = 440\,\mathrm{s}$, $\gamma_1 \approx 15{\cdot}7\,\mathrm{kP}$.

(2) Taking $\gamma_1 = 15{\cdot}7\,\text{kP}$ as a constant value, figure 8 shows a typical fit of equation (1) to the experimental amplitudes $\theta_0(t)$ within the harmonic approximation. Good agreement between experimental data and the theoretical relaxation curve is observed. For comparison, the dashed line in figure 8 shows the evolution of θ_0 calculated by assuming a homogeneous relaxation process driven by γ_1. The large discrepancy confirms, if necessary, that this possibility is definitely excluded. However, this first adjustment does not allow us to deduce a unique set of viscosity parameters. Fits of equivalent quality are obtained for

$$\left.\begin{aligned} -17{\cdot}0 \leqslant \alpha_2 \leqslant -15{\cdot}0\,\text{kP}, \\ 14{\cdot}0 \leqslant \eta_c \leqslant 18{\cdot}5\,\text{kP}, \\ -18{\cdot}0 \leqslant \alpha_1 \leqslant -8{\cdot}0\,\text{kP}. \end{aligned}\right\} \tag{17}$$

The uncertainties associated with the coefficients α_2 and η_c are in fact related to the uncertainty on the coefficient α_1: large values of $|\alpha_1|$ ($\alpha_1 = -18\,\text{kP}$) imply large values for $|\alpha_2|$ and $\eta_c(\alpha_2 = -17\,\text{kP})$ and ($\eta_c = 18{\cdot}5\,\text{kP}$). The small values for these coefficients correspond to a small value for $|\alpha_1|$. This is in order to keep the correct behaviour of the effective viscosity coefficient γ_{eff}. However, the variations of α_2 and η_c within these limits are not uncorrelated: all the best fits impose an accurate value for $\eta_{\text{bend}} = 0{\cdot}17 \pm 0{\cdot}02\,\text{kP}$, which is the viscosity coefficient which drives the reorientation at short times (see equation (8)). This value is found to depend only on the amplitude chosen for the initial fluctuation $\theta_0(0)$; decreasing $\theta_0(0)$ from 1° down to 0·01° induces values for η_{bend} smaller within a factor of two, but affects the values of α_2, η_c and α_1 by less than 5 per cent. Finally, as reported in the previous section, the sensitivity of the fit to the actual value of the ratio K_3/K_1 is very weak, and the value of K_1q^2 ranges between 0·5 and $2{\cdot}5\,\text{erg/cm}^3$. This last value is expected to be underestimated by a factor of about three (i.e. $1/\beta$ at the end of the relaxation).

(3) Substituting the viscosity coefficients in equation (1), and removing the harmonic approximation, allows us to calculate the time evolution of the initial fluctuation ($\theta_0(0) = 1°$) and to simulate the N.M.R. spectra for any time. Figure 9 shows, for a given set of viscosity parameters, the influence of the elastic parameters on the simulated lineshape for a given time. Figure 9 (*a*) shows the experimental spectrum recorded at $t = 210\,\text{s}$ ($\theta_0 = 65°$); a broad line is observed. Figures 9 (*b*), (*c*), (*d*) pictures the change in the simulated lineshape induced by increasing K_1q^2 from 0·5 to $7\,\text{erg/cm}^3$, keeping K_3/K_1 constant at a value of 0·3. The corresponding change in the distortion shape $\theta(z, t)$ is represented underneath for a quarter period $\lambda/4$. It is seen that an over-structured lineshape (corresponding to an over-square like distortion compared to the experimental one) is observed for small values of K_1q^2. Increasing K_1q^2 improves the simulated lineshape as well as rounding off the corresponding distortion, which means that the elastic energy is less confined in thin layers close to the nodes of the distortion. A similar effect is observed by increasing the ratio K_3/K_1; figures 9 (*e*), (*c*), (*f*), show the variation induced by increasing K_3/K_1 from 0·1 to 0·5, keeping K_1q^2 constant at $5\,\text{erg/cm}^3$. By comparing figures 9 (*f*) and (*d*), we observe that the sets $K_1q^2 = 7\,\text{erg/cm}^3$, $K_3/K_1 = 0{\cdot}3$ and $K_1q^2 = 5\,\text{erg/cm}^3$, $K_3/K_1 = 0{\cdot}5$ lead to quasi-identical simulations. It is no longer possible to distinguish between these combinations. Such a study, extended to the whole set of experimental spectra allows us to conclude that K_1q^2 is certainly in the range between 2 and $10\,\text{erg/cm}^3$ with the most probable values around 5–$7\,\text{erg/cm}^3$ and K_3/K_1 between 0·1 and 1 with the most

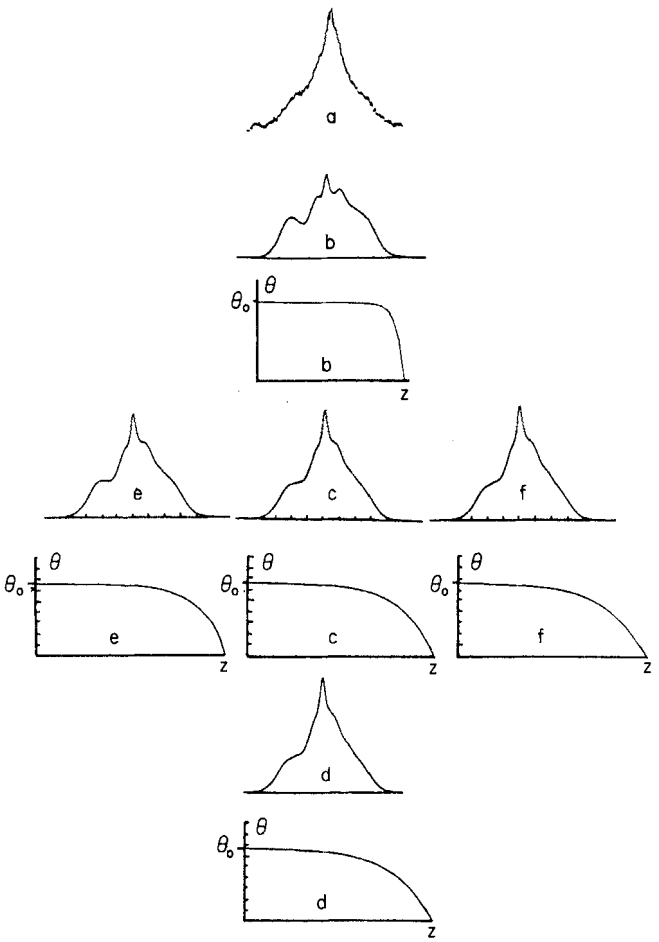

Figure 9. Spectra obtained at $t = 210$ s (*a*): experimental (*b–f*): calculated from equation (1) without the harmonic approximation (only the initial director distortion is assumed to be harmonic with $\theta_0(0) = 1°$). The viscosity coefficients are the same as in figure 8 and the elastic parameters are: (*b*) $K_1q^2 = 0{\cdot}5\,\mathrm{erg/cm^3}$, $K_3/K_1 = 0{\cdot}3$, (*c*) $K_1q^2 = 5\,\mathrm{erg/cm^3}$, $K_3/K_1 = 0{\cdot}3$, (*d*) $K_1q^2 = 7\,\mathrm{erg/cm^3}$, $K_3/K_1 = 0{\cdot}3$, (*e*) $K_1q^2 = 5\,\mathrm{erg/cm^3}$, $K_3/K_1 = 0{\cdot}1$, (*f*) $K_1q^2 = 5\,\mathrm{erg/cm^3}$, $K_3/K_1 = 0{\cdot}5$.

probable values around 0·3–0·5. These values allow us to check that $K_3q^2/\chi_a B^2$ is about 5–10 per cent as stated previously.

The simulation of the whole set of NMR spectra has imposed more restricted limited for the values of the viscosity parameters, than those deduced from simple fit of the amplitude $\theta_0(t)$. The final set of six viscoelastic parameters that are compatible with the simulations are

$$\left.\begin{aligned} \eta_{\mathrm{twist}} &= \gamma_1 = 15{\cdot}7\,\mathrm{kP}, \\ -16{\cdot}0 &\leqslant \alpha_1 \leqslant -10{\cdot}0\,\mathrm{kP}, \\ -16{\cdot}5 &\leqslant \alpha_2 \leqslant -15{\cdot}0\,\mathrm{kP}, \\ 15{\cdot}5 &\leqslant \eta_c \leqslant 18{\cdot}5\,\mathrm{kP}, \\ 0{\cdot}3 &\leqslant K_3/K_1 \leqslant 0{\cdot}5, \\ 5{\cdot}0 &\leqslant K_1q^2 \leqslant 7{\cdot}0\,\mathrm{erg/cm^3}. \end{aligned}\right\} \tag{18}$$

From these values the

$$\left.\begin{aligned} \eta_{\text{bend}} &= 0{\cdot}17 \pm 0{\cdot}02\,\text{kP}, \\ 6{\cdot}0 \leqslant \eta_{\text{splay}} &\leqslant 15{\cdot}7\,\text{kP}, \\ -17{\cdot}0 \leqslant \gamma_2 &\leqslant -15{\cdot}0\,\text{kP}, \\ 0{\cdot}16 \leqslant \eta_b &\leqslant 0{\cdot}30\,\text{kP}, \\ -0{\cdot}80 \leqslant \alpha_3 &\leqslant +0{\cdot}10\,\text{kP}, \end{aligned}\right\} \tag{19}$$

coefficients can be calculated. Figure 10 shows the experimental spectra ($T = 120°C$) as well as the simulated spectra computed at the corresponding times with $\alpha_1 = -13{\cdot}2\,\text{kP}$, $\alpha_2 = -15{\cdot}95\,\text{kP}$, $\eta_c = 16{\cdot}37\,\text{kP}$, $\gamma_1 = 15{\cdot}7\,\text{kP}$, $K_1 q^2 = 5\,\text{erg/cm}^3$ and $K_3/K_1 = 0{\cdot}5$. Very good agreement is obtained between the two sets. The small discrepancies which are observed can result from (i) different mechanisms of dissipation for the elastic energy, particularly by increasing the fundamental wavelength of the distortion $\lambda = (2\pi/q)$, as suggested by the observation of Platonov *et al.* [37] and (ii) the polydispersity of the sample. In this case, the average molecular mass may not be uniform within the sample. A small distribution of the values of the viscosity coefficients caused by this non-uniformity [20], could produce an extra broadening of the spectral lines [38], in particular in the range where rapid variation of the amplitude $\theta_0(t)$ is observed (see figure 8).

The time evolution of the distortion $\theta(z, t)$ corresponding to this set of parameters is shown figure 11. (a quarter of period ($\lambda/4$) is represented). Evolution towards a

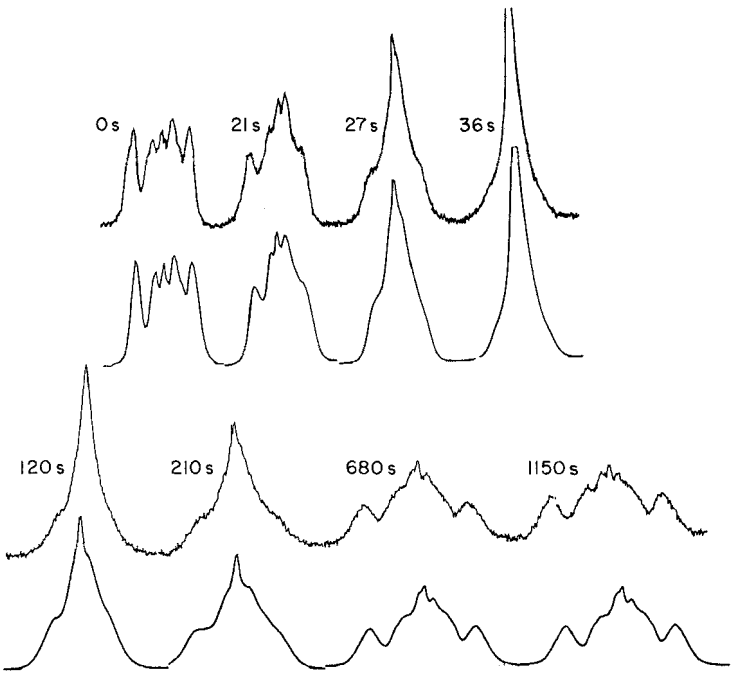

Figure 10. Experimental PMR spectra (upper) and simulated ones (lower) calculated from the evolution of an initial harmonic fluctuation ($\theta_0(0) = 1°$) through equation (1), without the harmonic approximation and the following parameters: $\alpha_1 = -13{\cdot}2\,\text{kP}$, $\alpha_2 = -15{\cdot}95\,\text{kP}$, $\eta_c = 16{\cdot}37\,\text{kP}$, $\gamma_1 = 15{\cdot}7\,\text{kP}$, $K_1 q^2 = 5\,\text{erg/cm}^3$, $K_3/K_1 = 0{\cdot}3$. Good agreement between the two sets is observed.

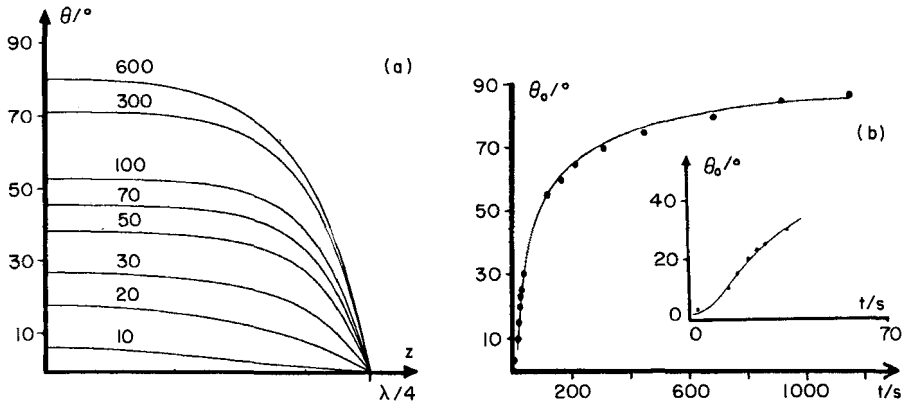

Figure 11. (*a*) Evolution of the distortion $\theta(z, t)$ over 1/4 of the period, corresponding to the set of parameters which achieves the simulation of figure 11. (times are in seconds) (*b*) the solid line is the corresponding evolution of the maximum $\theta_0(t)$. Note the (small) difference with the evolution of figure 8 determined within the harmonic approximation.

square distortion is observed. However, for $\theta_0(t) \approx \pi/2$, this distortion remains far from a pure square distortion. As a consequence, the corresponding experimental spectrum (see figure 10) is slightly different from the initial aligned spectrum (see figure 4(*a*).

Finally, integrating equation (2) numerically provides the velocity profile $v_x(z, t)$ as shown in figure 12 (as in figure 11, only a quarter of the period $\lambda/4$ is represented). This profile is found to evolve from a sinusoidal (due to the initial definition of the distortion) to a zig-zag shape: at the end of the relaxation, the velocity varies practically linearly over the half period of distortion. The velocity and the orientational fields are in quadrature. Two extreme situations appear (i) for the domains corresponding to the maximum of the distortion, the velocity is always zero, (ii) for the domains located at the node of the distortion, the velocity is a maximum and reaches at $t = 20$ s a value of $0{\cdot}45 \times 10^{-2}\ \lambda$/s. The maximum distance covered by the fluid close to the nodes during the reorientation can be evaluated to be $d \sim \lambda/2$. So, the proposed method not only allows us to determine the viscosity coefficients but

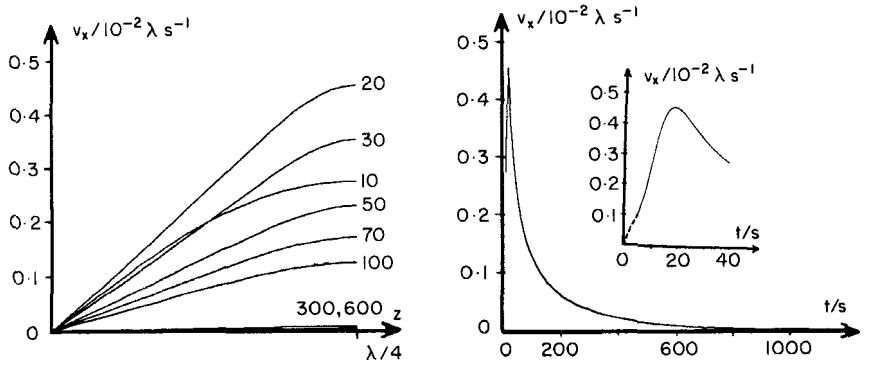

Figure 12. (*a*) Evolution of the velocity profile over 1/4 of period ($\lambda\,s^{-1}$ units) calculated from equation (2) with the same set of parameters as used in figure 10 (the times are in seconds) (*b*) corresponding evolution of the maximum velocity v_x at the nodes of the distortion. The inset is a magnification at short times.

also leads to information about the distortion and velocity pattern during the relaxation. In the next section, we discuss the values found for the various viscoelastic parameters.

6. Discussion

6.1. *Elastic constants*

The ratio K_3/K_1 is found to be smaller than unity. According to the theoretical predictions of de Gennes [39] and Meyer [40], this result agrees with the semiflexible nature of the polymer. The value $K_3/K_1 \approx 0{\cdot}3$–$0{\cdot}5$ is close (but larger) to that estimated for a main-chain thermotropic polymer with different mesogenic unit and five methylene groups in the spacer $\sim 0{\cdot}1$ [14], and comparable to the values obtained for lyotropic nematic polymers (PBLG $\sim$ 1·17 [12], and the PBT $\sim$ 0·44 [13]).

The value $K_1 q^2 \sim 5$–$7\,\text{erg/cm}^3$ supports the estimate of the distortion wavelength obtained from the optical observations: a typical value for $K_1 \approx 10^{-6}$ dyne [31] leads to $\lambda \approx 60$–$80\,\mu$m comparable to $\lambda \approx 50$–$80\,\mu$m deduced from the optical measurement, for a polymer of larger molecular mass.

6.2. *Viscosity coefficients*

As noted in the previous experimental studies of polymeric systems [12, 13, 16], and according to the theoretical predictions developed mainly for rod-like polymers [10, 11], we have also found for our main-chain polymer that the viscosity coefficients can be classified into two groups. On one hand, those which are of the same order of magnitude as γ_1, namely α_2, η_c, α_1, γ_2 whose average values (at $T = 120°C$) are typically 10^6 larger than the corresponding values reported for low molar mass nematics [41]. On the other hand, the coefficients which are smaller than γ_1 by a factor 10 to 10^2 namely η_b, η_{bend}, α_3. These results agree with the theoretical models of de Gennes [39] and Meyer [40] where γ_1, γ_2, η_c and α_1 are predicted to diverge as the chain length increases, whereas α_3 and η_b reach finite values.

The value of α_2 is negative as expected for calamitic liquid crystals [42]. However, it is difficult to derive from our experiment the actual sign of the coefficient α_3 which determines the flow behaviour of the material [42, 43]. It can be noted, that positive values for α_3 have been determined for few compounds which generally exhibit, at low temperature, a nematic to smectic transition [44, 45]. Such a transition does not exist for our system, so that the coefficient α_3, according to its average value within the measured limits (equations (19)), is probably negative. In this case, the value derived for the ratio α_3/α_2 is smaller than 0·07 which implies a flow alignment angle ϕ, given by $\text{tg}^2\,\phi = \alpha_3/\alpha_2$, smaller than 15°. This value is comparable to that measured for 4,4′-dimethoxyaxzoxy benzene, a low molar mass nematic whose chemical formula is rather similar to that of the mesogenic unit of our polymer: $\phi = 17°$ at $T = 125°C$ [46].

The ratio $\eta_{splay}/\eta_{twist}$ ranges between 0·4 and 1. The value 0·4 is significantly smaller than that measured in lyotropic systems ($\sim 0{\cdot}85$ [35], ~ 1. [12]) and in low molar mass nematics ($\sim 1 \pm 0{\cdot}01$ for 4-*n*-pentyl-4′-cyanobiphenyl [47]). It must be noted that a value close to unity implies, in our case, values for the coefficient $|\alpha_1|$ smaller than γ_1, which is a situation predicted by the theories relative to rod-like polymers [10, 11]. According to these considerations, α_1 is not only negative but probably such that $|\alpha_1| < \gamma_1$.

The coefficient η_{bend}, as we have seen, is accurately determined from the fit. Its value is found to be close (smaller) to that of the second Miesowicz coefficient η_b [19]. On the other hand, a viscosity coefficient η_s measured under shear in the nematic phase for the AZA9 polymer has been recently reported by Blumstein *et al.* [2]. At high shear rate, a macroscopic alignment of the director is observed. Consequently, the values of η_s extrapolated to zero frequency ω, are expected to be close to η_b. A typical value of $\eta_s(\omega \to 0)$ at 130°C is 0·06 kP, measured for the polymer AZA9 ($\bar{M}_n = 5200$) [2]. Assuming a weak variation of this coefficient with chain length [39], and a stronger variation with temperature, this value can be compared roughly to $\eta_b \approx 0{\cdot}16$–$0{\cdot}30$ kP estimated with the present method at 120°C for the AZA9d14 polymer. The two coefficients are of the same order of magnitude.

Finally, the acceleration time τ_{acc} can be estimated. Its value is of the order of $\rho d^2/\eta_{bend}$ where ρ is the density and d is a characteristic distance in the system. Two such distances are the tube diameter and the wavelength of the distortion. In both cases, τ_{acc} is very small (milliseconds or less) compared to the acquisition time of the first NMR spectrum, supporting the assumption leading to equations (1 and 2).

7. Conclusion

Here we have presented a detailed procedure to measure viscoelastic coefficients using the NMR method proposed previously in [16]. For the particular case of the main-chain thermotropic polymer studied in this paper, optical observations clearly show that the reorientation process following rotation of a nematic monodomain through an angle $\alpha \approx \pi/2$ with respect to the direction of the magnetic field, involves a periodic pure bend distortion. The model developed in [16], coupled with an accurate analysis of the NMR lineshapes allows the description of the reorientational pattern. Because NMR is strongly sensitive to the local disorientation of the director field, it appears as an useful tool to characterize the shape of the distortion, as well as its time evolution. However, the present analysis does not explain the mechanism of selection of the wavevector **q** (modulus and direction) of the initially amplified fluctuation of the director. The lineshape analysis allows us to determine the viscosity parameters and to evaluate the elastic contribution more precisely than in [16]. The measured elastic parameters support the semiflexible nature of the polymer studied whereas the viscosity coefficients reveal a strong anisotropy. This strong anisotropy emphazises the liquid-crystalline nature of the nematic polymer and is probably the driving factor for the reorientation processes through a periodic transient distortion. Thus, such processes are expected to happen as soon as an external oscillation (electric or magnetic field, shear) is applied to a nematic phase and induces reorientation. In particular, this can be a route to describe the time dependence of the alignment process leading from a polydomain structure to a monodomain. Such a study is currently underway in our laboratory.

Finally, it must be recognized that the results obtained by this NMR method, and in particular the values of the viscoelastic parameters, depend in an essential manner on the theoretical mode used. Consequently, they may still be questionable because systematic errors due to a possible limitation of the model cannot be estimated. Confirmation (or refutation) of these results by other, and if possible, more direct methods is highly desirable. So far, no such method has been proposed for this kind of nematic polymer. It is hoped that this work will stimulate the development of such new methods.

We are indebted to Dr. J. F.d'Allest for the synthesis of the partially deuteriated polymer samples.

References

[1] BAIRD, D. G., and BALLMAN, R. L., 1979, *J. Rheol.*, **23**, 505.
[2] BLUMSTEIN, A., THOMAS, O., and KUMAR, R. S., 1986, *J. Polym. Sci. Polym. Phys. Ed.*, **24**, 27.
[3] ONOGI, and ASADA, T., 1980, *Rheology*, Vol. I, edited by G. Astarita, G. Marucci and L. Nicolais (Plenum), p. 127.
[4] WISSBRUN, K. F., 1981, *J. Rheol.*, **25**, 619. WISSBRUN, K. F., and GRIFFIN, A. C., 1982, *J. Polym. Sci. Polym. Phys.* Ed., **20**, 1835.
[5] FRANK, F. C., 1958, *Discuss. Faraday Soc.*, **25**, 19.
[6] ERICKSEN, J. F., 1962, *Archs ration. mech. Anal.*, **9**, 371.
[7] LESLIE, F. M., 1968, *Archs ration. mech. Anal.*, **28**, 265.
[8] PARODI, O., 1970, *J. Phys., Paris*, **31**, 580.
[9] MARUCCI, G., 1982, *Molec. Crystals liq. Crystals*, **72** 153.
[10] KUZUU, N., and DOI, M., 1983, *J. phys. Soc. Japan*, **52**, 3486; 1984, *Ibid.*, **53**, 1031.
[11] LEE, S. D., and MEYER, R. B., 1986, *J. chem. Phys.*, **84**, 3443.
[12] TARATUTA, V. G., HURD, A. J., and MEYER, R. B., 1985, *Phys. Rev. Lett.*, **55**, 246.
[13] KAZUNARI, S. E., and BERRY, G. C., 1987, *Molec. Crystals liq. Crystals*, **153**, 133.
[14] SUN-ZHENG-MIN, and KLEMAN, M., 1984, *Molec. Crystals liq. Crystals*, **111**, 321.
[15] ESNAULT, P., VOLINO, F. MARTINS, A. F., KUMAR, S., and BLUMSTEIN, A., 1987, *Molec. Crystals liq. Crystals*, **153**, 145.
[16] MARTINS, A. F., ESNAULT, P., and VOLINO, F., 1986, *Phys. Rev. Lett.*, **57**, 1745.
[17] FILAS, R. W., HADJO, L. E., and ERINGEN, A. C., 1974, *J. chem. Phys.*, **61**, 3037.
[18] ORWOLL, R. D., and VOLD, R. L., 1975, *J. Am. chem. Soc.*, **93**, 5395.
[19] DE GENNES, P. G., 1974, *The Physics of Liquid Crystals* (Clarendon Press).
[20] KLEIN, T., HONG-XI-JUN, ESNAULT, P., BLUMSTEIN, A., and VOLINO, F., 1989, *Macromolecules*, **22**, 3731.
[21] BROCHARD, F., GUYON, E., and PIERANSKI, P., 1973, *J. Phys., Paris*, **34** 35.
[22] GUYON, E., MEYER, R. B., and SALAN, J., 1979, *Molec. Crystals liq. Crystals*, **54**, 261.
[23] LONGBERG, F., and MEYER, R. B., 1985, *Phys. Rev. Lett.*, **55**, 718.
[24] KUZMA, M. R., 1986, *Phys. Rev. Lett.*, **57**, 349.
[25] FRADEN, S., HURD, A. J., MEYER, R. B., CANOON, M., and CASPAR, D. L., 1985, *J. Phys., Paris*, **46**, C385.
[26] (a) SRAJER, G., FRADEN, S., and MEYER, R. B., 1988, *Phys. Rev. Lett.*, **61**, 889. (b) MARTINS, A. F., ESNAULT, P., and VOLINO, F., 1988, *Phys. Rev. Lett.*, **61**, 900.
[27] BLUMSTEIN, A., VILASAGAR, S., PONRATHNAM, S., CLOUGH, S. B., MARET, G., and BLUMSTEIN, R. B., 1982, *J. Polym. Sci. Polym. Phys. Ed.*, **20**, 887.
[28] VAN DOORN, C. Z., 1975, *J. Phys., Paris*, **36**, C1-261.
[29] CLARK, M. G., and LESLIE, F. M., 1978, *Proc. R. Soc.* A, **361**, 463.
[30] ORSAY LIQUID CRYSTAL GROUP, 1969, *J. chem. Phys.*, **51**, 816.
[31] ESNAULT, P., CASQUILHO, J. P., and VOLINO, F., 1988, *Liq. Crystals*, **3**, 1425.
[32] LIN, W. J., and FREED, J. H., 1979, *J. chem. Phys.*, **83**, 379.
[33] ESNAULT, P., 1988, Ph.D. Thesis, University of Grenoble.
[34] ESNAULT, P., GALLAND, D., VOLINO, F., and BLUMSTEIN, R. B., 1989, *Macromolecules*, **22**, 3734.
[35] MARTINS, A. F., FERREIRA, J. B., VOLINO, F., BLUNSTEIN, A., and BLUMSTEIN, R. B., 1983, *Macromolecules*, **16**, 279.
[36] VOLINO, F., and BLUMSTEIN, R. B., 1984, *Molec. Crystals liq. Crystals*, **113**, 147.
[37] PLATONOV, V. A., LITOVCHENKO, G. D., BELOUSOVA, T. A., MIL'KOVA, L. P., KUMKICHIKHIN, M. V., and PAPKOV, S. P., 1976, *Poly. Sci. U.S.S.R.*, **18**, 256.
[38] CASQUILHO, J. P., 1990, Thesis, University Nova of Lisbon, Portugal.
[39] DE GENNES, P. G., 1982, *Polymer Liquid Crystals*, edited by W. Krigbaum, A. Ciferri and R. B. Meyer (Academic Press), Chap. 5.
[40] MEYER, R. B., 1982, *Polymer Liquid Crystals*, edited by W. Krigbaum, A. Ciferri and R. B. Meyer (Academic Press), Chap. 6.

[41] (a) GÄHWILLER, CH., 1973, *Molec Crystals liq. Crystals*, **20**, 301. (b) DIOGO, A. C., and MARTINS, A. F., 1981 *Molec Crystals liq. Crystals*, **66**, 133.
[42] CARLSSON, T., 1982, *Molec. Crystals liq. Crystals*, **89**, 57.
[43] MARUCCI, G., 1983, *Pure appl. Chem.*, **7**, 1545.
[44] KNEPPE, H., SCHNEIDER, F., and SHARMA, N. K., 1981, *Ber. Bunsenge phys. Chem.*, **85**, 784.
[45] CLADIS, P. E., and TORZA, S., 1975, *Phys. Rev. Lett.*, **35**, 1283.
[46] ORSAY LIQUID CRYSTAL GROUP, 1971, *Molec. Crystals liq. Crystals*, **13**, 187.
[47] COLES, H. J., and SEFTON, M. S., 1985, *Molec. Crystals liq. Crystals Lett.*, **3**, 63.
[48] SRAJER, G., FRADEN, S., and MEYER, R. B., 1989, *Phys. Rev.* A, **39**, 4828.
[49] REY, A. D., and DENN, M. M., 1989, *Liq. Crystals*, **4**, 409.